Research Article

Kinetic Study of Calcium Phosphate Precipitation in the System H$_3$PO$_4$-Ca(OH)$_2$-H$_2$O at 30°C

K. Labgairi [ID],[1] A. Borji [ID],[1,2] M. Kaddami [ID],[1] and A. Jourani [ID][1]

[1]*Hassan First University of Settat, Faculty of Sciences and Techniques, Laboratory of Physical Chemistry of Processes and Materials, BP 577, Settat, Morocco*
[2]*Department of Process Engineering and Food Techniques, Hassan II Institute of Agronomy and Veterinary Sciences (IAV), BP 6202, Rabat, Morocco*

Correspondence should be addressed to A. Borji; abdlali.borji@gmail.com

The precipitation kinetics of calcium phosphates, namely, hydroxyapatite (HAP), dicalcium phosphate dihydrate (DCPD), dicalcium phosphate anhydrous (DCPA), and monocalcium phosphate monohydrate (MCPM), were studied at 30°C by mixing calcium hydroxide, water, and phosphoric acid. The studied mixture was selected according to the stability domain of different calcium phosphates by referring to the phase diagram of the ternary system of H$_3$PO$_4$-Ca(OH)$_2$-H$_2$O at 30°C. The precipitation reaction has been monitored by following the changes in the conductivity, pH, and calcium concentration. The solid phases formed at different stages of this precipitation were characterized by X-ray diffraction.

1. Introduction

Calcium phosphates have been extensively studied by many researchers and for diverse interests because of their fundamental and applied importance, where they are involved in different domains: chemistry, biology, agronomy, food processing, etc. However, the precipitation of the calcium phosphates is very complex, and the compounds of calcium phosphate formed depend significantly on the operating conditions [1]. The precipitation of calcium phosphates was studied by several authors under different conditions [2–6]. In a previous work, the isotherm of the quasi-ternary system Ca(OH)$_2$-H$_3$PO$_4$-H$_2$O has been established at 30°C [7]. Crystallization fields of CaHPO$_4$. 2H$_2$O, CaHPO$_4$, and Ca(H$_2$PO$_4$)$_2$. H$_2$O have been established. The domains of the coexistence of solid-liquid (Ca$_{10}$(PO$_4$)$_6$(OH)$_2$-liquid, CaHPO$_4$. 2H$_2$O-liquid, CaHPO$_4$-liquid, and Ca(H$_2$PO$_4$)$_2$. H$_2$O-liquid) as well as of two solids-liquid (Ca$_{10}$(PO$_4$)$_6$(OH)$_2$ plus CaHPO$_4$. 2H$_2$O-liquid and CaHPO$_4$ plus Ca(H$_2$PO$_4$)$_2$. H$_2$O-liquid) are also defined.

Ferreira et al. [5] studied the precipitation of dicalcium phosphate dihydrate in a closed system at 25°C by mixing a calcium hydroxide suspension and a phosphoric acid solution in equimolar amounts. The concentration of calcium hydroxide and phosphoric acid, before mixing, varies from 50 to 300 mmol/dm^3. This study demonstrated that the process of precipitation of brushite may be divided into five stages. The first phase precipitated is hydroxyapatite (Ca$_{10}$(PO$_4$)$_6$OH)$_2$, while the steady phase is brushite (DCPD). Chaair et al. [8] found that, during the precipitation of hydroxyapatite (Ca/P = 1.667), several steps are observed, particularly during the first two hours of precipitation. The results obtained during the first minutes of the precipitation show that an amorphous solid is formed and converted into an apatite phase. Ca/P increases during the time until it stabilizes at a value of 1.667, corresponding to stoichiometric hydroxyapatite. Jourani and Bounahmidi [9] studied the spontaneous precipitation of calcium phosphate in the conditions of purification of cane juice. They showed that the precipitation takes place in two steps. The first step is very fast and corresponds to the formation of amorphous calcium phosphate and dicalcium phosphate dihydrate, while the second step takes place with the transformation of the first-formed precipitates to

TABLE 1: pH precipitation range of some calcium phosphates [11–14].

Abbreviation	Chemical formula	Ca/P	Preparation conditions
Precipitates			pH
MCPM	$Ca(H_2PO_4)_2 \cdot H_2O$	0.5	0–2
DCPD	$CaHPO_4 \cdot 2H_2O$	1	2–6
HAP	$Ca_{10}(PO_4)_6(OH)_2$	1.67	9.5–12
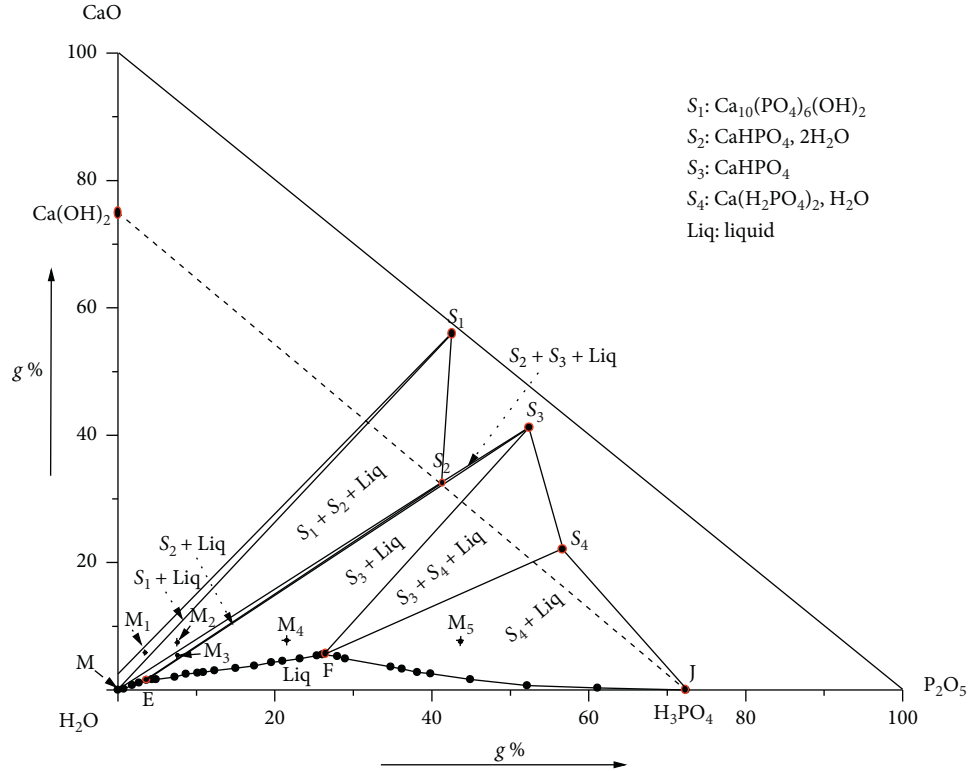
FIGURE 1: Solubility diagram of the $Ca(OH)_2$-H_3PO_4-H_2O quasi-ternary system at 30°C [7]. ME, EF, and FJ are the solubility branches of solids $S2$, $S3$, and $S4$. $M1$–$M5$ represent the composition of experimental mixtures according to Table 2.

hydroxyapatite. On the contrary, Rabadjieva et al. [10] showed that the preparation of calcium phosphates, which precipitate, strongly depends on pH of the medium. Table 1 shows these different calcium phosphates with their stabilization pH ranges [11–14].

Another work [15] was devoted to the preparation of the synthetic powder of hydroxyapatite by the reaction between $Ca(OH)_2$ and H_3PO_4 following the wet precipitation technique and considering several parameters, namely, the reaction temperature (30°C, 50°C, and 85°C), the acid addition rate (slow and fast acid addition rates), and the heat treatment temperature (950°C and 1250°C). This study showed that the properties of the final product can be shaped depending on the influence of process parameters.

In more recent work [16], Rabadjieva et al. showed that the coprecipitation of dicalcium phosphate dihydrate (DCPD) and hydroxyapatite (HA) occurs at pH 4, while at pH > 4, the stable phase is DCPD. This work also showed that the conversion of dicalcium phosphate to hydroxyapatite strongly depends on the residence time of the precipitate in the stock solution.

TABLE 2: Compositions of studied mixtures.

Mixture	Composition of the initial mixture ($g\%$)					
	Quasi-ternary system H_3PO_4-$Ca(OH)_2$-H_2O			Ternary system CaO-P_2O_5-H_2O		
	$Ca(OH)_2$	H_3PO_4	H_2O	CaO	P_2O_5	H_2O
M_1	7.50	5.00	87.50	5.68	3.62	90.70
M_2	10.00	10.20	79.80	7.57	7.38	85.05
M_3	7.50	10.00	82.50	5.68	7.24	87.08
M_4	10.00	30.00	60.00	7.57	21.72	70.71
M_5	10.00	60.00	30.00	7.57	43.44	48.99

In this context and following the work carried out in our laboratory, in which the isotherm of the ternary system $Ca(OH)_2$-H_3PO_4-H_2O at 30°C [7] has been performed, the aim of this study is to conduct a kinetic study in the same system and follow the stages of the precipitation before obtaining the stable phase expected by the phase equilibrium diagram. This will allow us to bring out the intermediate phases and to understand better the formation of the most stable phase according to the operating conditions.
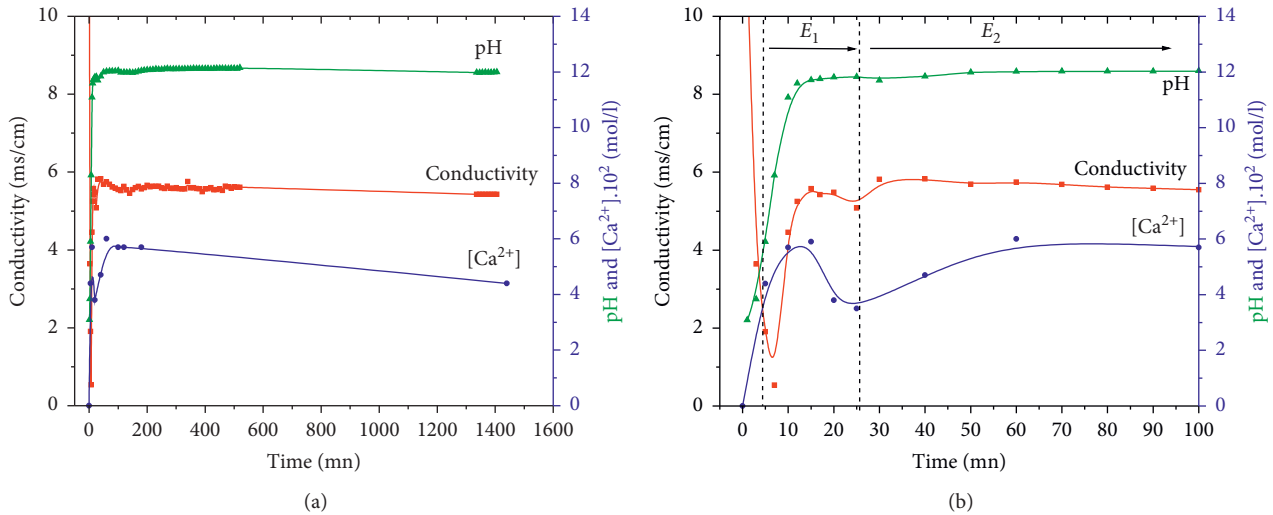
FIGURE 2: (a) Evolution of the conductivity, pH, and Ca^{2+} concentration for mixture $M1$. (b) Evolution of the conductivity, pH, and Ca^{2+} concentration relative to mixture $M1$ during the first 100 minutes.

2. Materials and Methods

The experimental setup used in this study consists of a jacketed reactor with the magnetic stirrer, a thermostatic bath for temperature control, and a conductimeter and a pH meter for conductivity and pH measurements, respectively. The precipitation reaction of calcium phosphate was carried out by mixing of well-defined quantities of calcium hydroxide, phosphoric acid, and distilled water. The experiments were performed at 30°C. According to the ternary diagram of H_3PO_4-$Ca(OH)_2$-H_2O and to the stability domain of HAP, DCPD and HAP, DCPD, DCPA, and MCPM, respectively (see Figure 1), the compositions of studied mixtures $M1$, $M2$, $M3$, $M4$, and $M5$ of a total mass of 50 g (Table 2) have been selected.

In order to study the kinetics of this precipitation, calcium hydroxide was rapidly added to the phosphoric acid solution. pH and conductivity of the mixture were monitored during that time. The variation of calcium concentration as a function of time has been determined by taking the samples and measuring their calcium concentration after their filtration in vacuum by complexometry using EDTA. The formed solids were removed at different time intervals, dried, and identified by X-ray diffraction.

3. Results and Discussion

3.1. Hydroxyapatite Stability Domain (Mixture M1). The evolution of pH, conductivity, and Ca^{2+} concentration, as a function of time, related to mixture $M1$ (Table 2), is shown in Figure 2(a). In order to better visualize the evolution of the precipitation during the first instants, Figure 2(b) shows the evolution of conductivity, pH, and Ca^{2+} concentration during the first 100 minutes.

As can be seen in Figure 2(b), the Ca^{2+} concentration and pH increase during the first eight minutes further to the dissolution of lime. However, the solution conductivity decreases revealing the precipitation of calcium phosphate.

Then, this conductivity increases until a certain value and decreases slightly and then increases before declining marginally. In this time interval, the calcium concentration follows the same variations as the conductivity, but pH remains practically constant.

Solid samples were characterized by X-ray diffraction at 5, 10, 20, 40, and 2160 min (36 h) (see Figure 3). The X-ray diffraction diagram of solids taken at 5 (Figure 3(a)), 10 (Figure 3(b)), and 20 min (Figure 3(c)) shows the existence of DCPD, HAP, and $Ca(OH)_2$. The X-ray diffraction diagram of the solid removed at 40 min (Figure 3(d)) shows the presence of DCPD and HAP. However, we find that the solid formed at 2160 min is HAP (Figure 3(e)).

Based on these data, we can conclude that the first precipitation step is the formation of DCPD and the nucleation of HAP with the presence of $Ca(OH)_2$, which is not yet dissociated.

Indeed, in the first 8 minutes, pH of the medium is in the range 3–6, which corresponds to the stability domain of DCPD [11–14]. On the contrary, according to Rabadjieva et al. [16], the coprecipitation of DCPD and HAP occurs at pH 4. The increase in conductivity between 8 and 15 min is explained by the continuous dissolution of calcium hydroxide and by the dissolution of brushite because pH exceeds the range of stability of DCPD (pH > 7). This results in an increase in the calcium concentration, and therefore, the formation of HAP is continued. That is why we see a decrease in conductivity and calcium concentration between 15 and 25 min. Then, DCPD is transformed as one goes along into HAP [16]. The presence of calcium carbonate with HAP is probably due to contamination by atmospheric CO_2 during separation.

3.2. Stability Domain of DCPD and HAP (Mixture M2). Figure 4 represents the evolution of pH, conductivity, and concentration of Ca^{2+} versus time, relative to mixture $M2$. The conductivity relative to mixture $M2$ (see Figure 4),
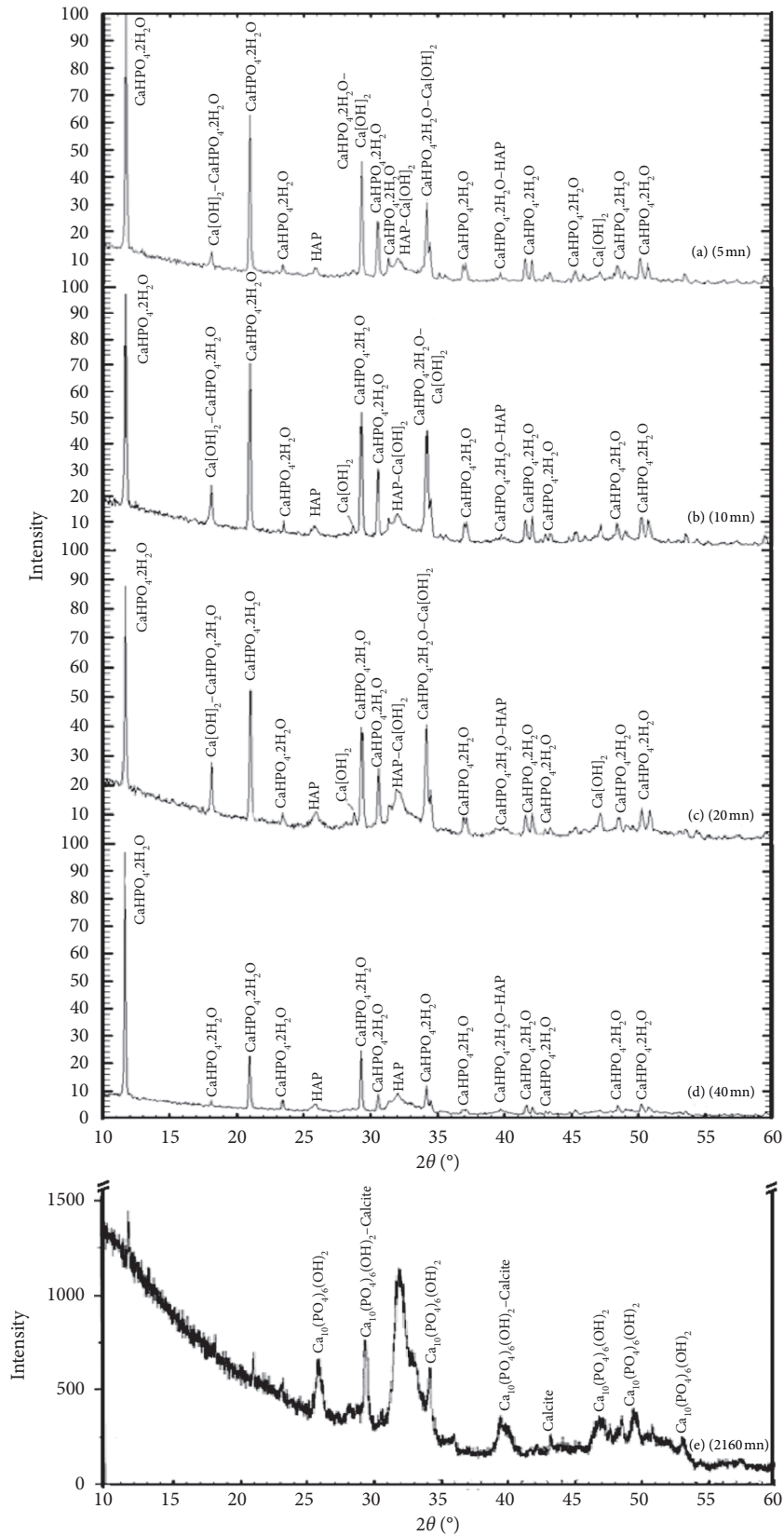
Figure 3: X-ray diagrams of the solid phase taken from mixture $M1$ as a function of time: (a) at 5 min, (b) at 10 min, (c) at 20 min, (d) at 40 min, and (e) at 2160 min.
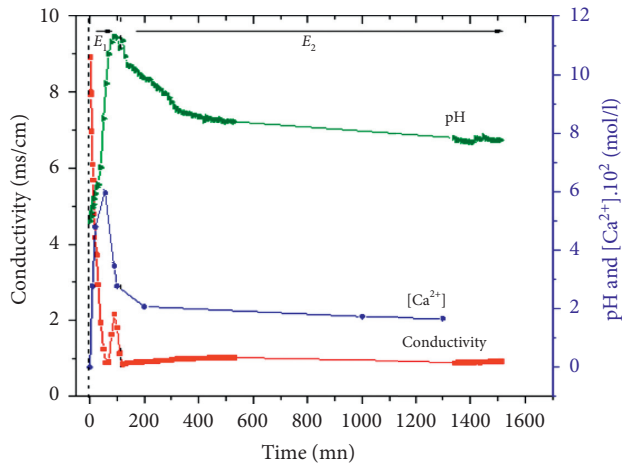
FIGURE 4: Evolution of the conductivity, pH, and Ca^{2+} concentration for mixture $M2$.

corresponding to the domain of stability of DCPD and HAP (see Figure 1), decreases brutally between 0 and 60 minutes, then it increases rapidly and decreases around 100 minutes, and then it stabilizes. pH increases rapidly from the first moments until a maximum, then decreases between 100 and 300 minutes, and then, it decreases slowly. The calcium concentration evolves in parallel to the evolution of pH.

To explain these variations, the samples have been taken at 5, 100, and 1200 minutes and filtered. The solid phases were analyzed by X-ray diffraction.

In Figure 5(a), the diagram of the X-rays of the solid taken at 5 min is shown. This diagram shows the existence of DCPD and $Ca(OH)_2$.

The X-ray diagram of the solid taken at 100 min (Figure 5(b)) shows the existence of DCPD with a low proportion of HAP.

The X-ray diagram of the solid taken at 1200 min (Figure 5(c)) shows the presence of a mixture of DCPD and HAP.

During the first step (0–60 min), DCPD is formed according to the following equation [5]. This explains the decrease in conductivity.

$$Ca(OH)_2 + H_3PO_4 \longrightarrow CaHPO_4 \cdot 2H_2O \qquad (1)$$

This is quite normal because pH of the medium is between 5 and 6 for this step, which corresponds to the range stability of DCPD ($2 < pH < 6$). However, in this step, we do not have the formation of HAP because pH is higher than 4 [16].

At the start of the second step (after 60 min), pH is higher than 9, which corresponds to the domain of the formation of HAP (Figure 5(b)), and since DCPD is unstable at this pH, it has dissociated. This explains the increase in conductivity and the concentration of Ca^{2+} and the decrease in pH. Then, HAP continues to form to obtain, at the end, a mixture of DCPD and HAP for pH between 7 and 8 (Figure 5(c)).

3.3. Stability Domain of DCPD (Mixture M3).
The curves of pH, conductivity, and Ca^{2+} concentration as a function of time, related to mixture $M3$, are shown in Figure 6. This

figure shows a decrease of the conductivity followed by an increase, and the latter begins again to decrease until the equilibrium; for pH, it is shown to increase until a maximum value and then decreases slowly, and it sudden drops before reaching the equilibrium. The Ca^{2+} concentration evolves in parallel to the evolution of pH.

To explain these steps, samples at 5, 15, 200, and 630 min have been taken and filtered, and the solids have been analyzed by X-ray diffraction. The corresponding diagrams are given in Figure 7.

The X-ray diagrams of the solids taken at 5 and 15 min (Figures 7(a) and 7(b)) show the existence of a mixture of DCPD, HAP, and $Ca(OH)_2$. However, the X-ray diagram of the solid taken at 200 min (Figure 7(c)) and that of the solid taken at 630 min (Figure 7(d)) show the existence of DCPD alone.

It is noted that DCPD and HAP are formed during Step 1, where pH of the medium is between 3 and 5 [11–14, 16], with the existence of $Ca(OH)_2$ which has not yet completely dissociated. This explains the decrease in conductivity during this step. However, the increase in pH and calcium concentration is due to the dissolution of calcium hydroxide, which causes the dissolution of part of DCPD which is unstable at this pH. This explains the increase in conductivity at the end of this step. Then, the formation of DCPD is continued in the second step, which decreases the conductivity, pH, and calcium concentration, and consequently leads to the transformation of the HAP formed into DCPD.

3.4. Stability Domain of DCPA (Mixture M4).
The variation of pH, conductivity, and Ca^{2+} concentration as a function of time, relative to mixture $M4$, is shown in Figure 8. As can be seen in this figure, the conductivity decreases from its initial value and reaches a plateau from 500 min. pH decreases rapidly from the first instants and remains constant at the value of 2.5; this is the pH value where DCPA is more stable. The concentration of Ca^{2+} increases until it reaches a maximum value and then it slowly decreases. This shows that this precipitation takes place in a single step. The X-ray diagram (Figure 9) shows the formation of DCPA without the existence of another phase.

3.5. Stability Domain of MCPM (Mixture M5).
The evolution of pH, conductivity, and Ca^{2+} concentration as a function of time relative to mixture $M5$, is shown in Figure 10. Analysis of these curves indicates that pH and conductivity decrease rapidly during the first few minutes. Then, the conductivity decreases very slightly, while pH remains constant (pH < 2 is the stability range of MCPM). The Ca^{2+} concentration increases rapidly following the dissolution of $Ca(OH)_2$, until it reaches a maximum value around 30 minutes, and then it slowly decreases. This confirms that this precipitation takes place in a single step.

In order to identify the solid phase which appears, several samples have been taken at various moments and filtered. The solid phases were analyzed by X-ray diffraction.
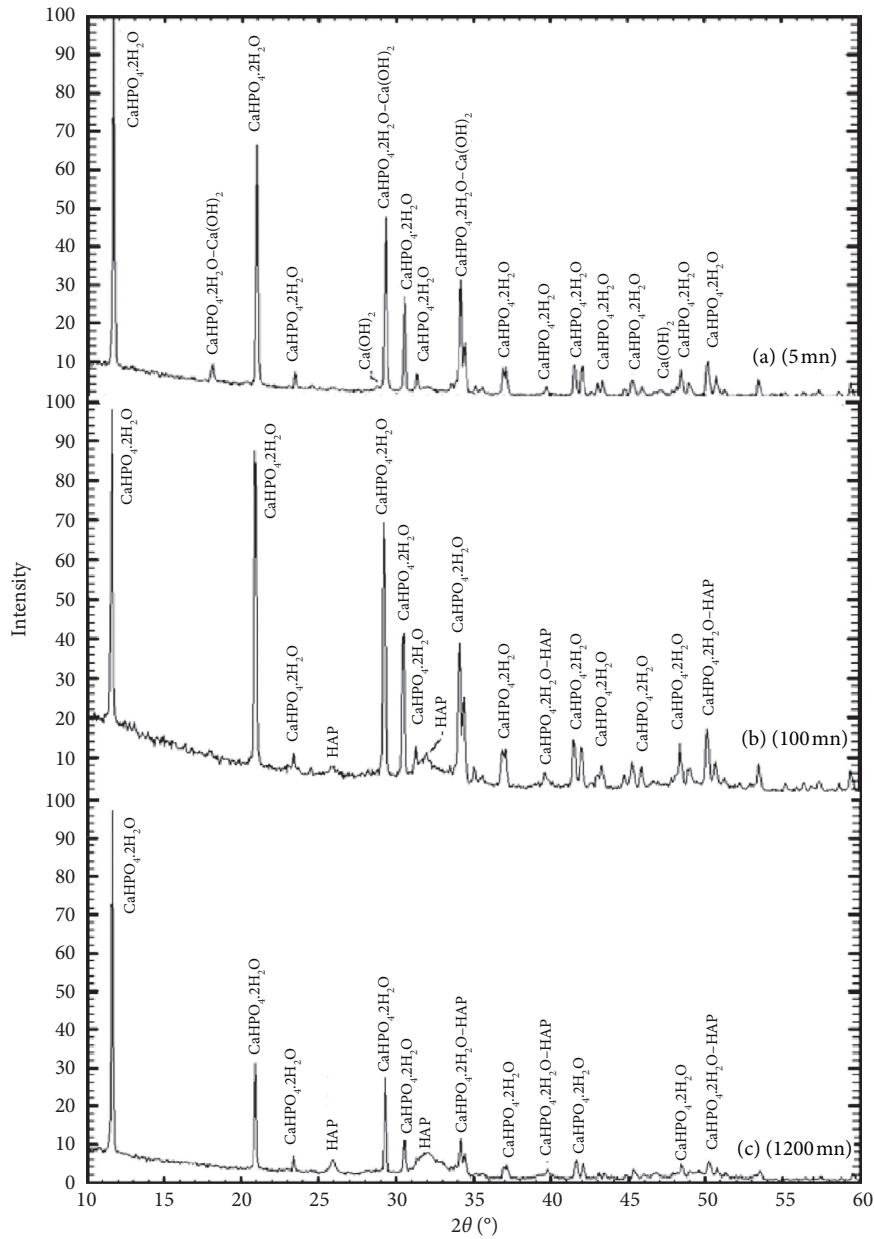
Figure 5: X-ray diagrams of the solid phase taken from the $M2$ mixture as a function of time: (a) at 5 min, (b) at 100 min, and (c) at 1200 min.
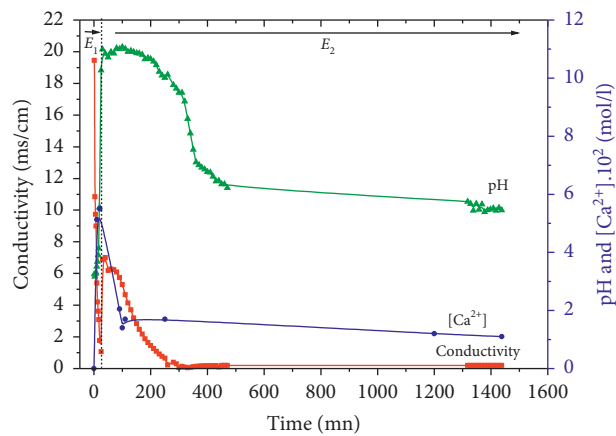

Figure 6: Evolution of the conductivity, pH, and Ca^{2+} concentration versus time relative to mixture $M3$.
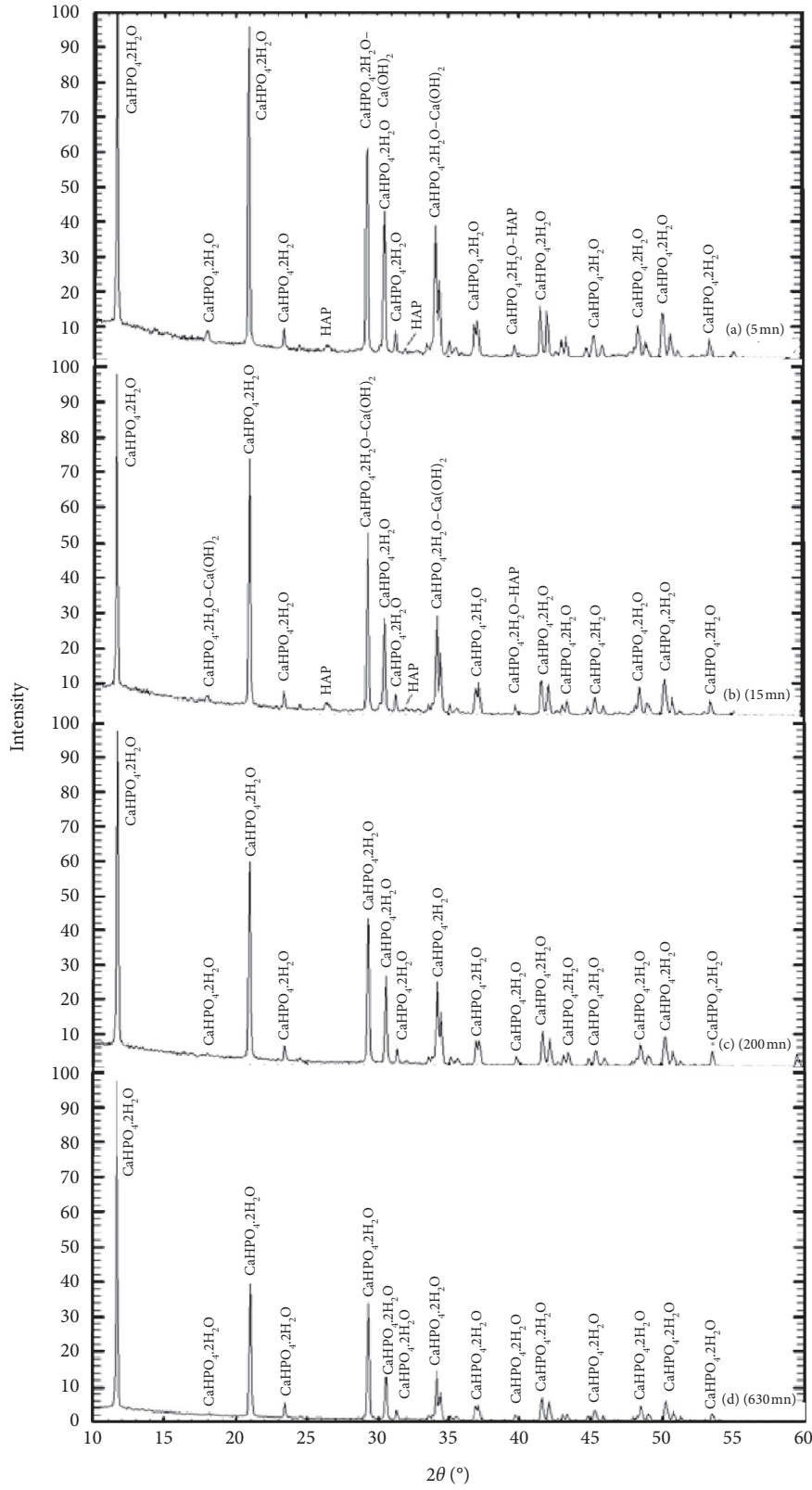
FIGURE 7: X-ray diagrams of the solid phase taken from mixture $M3$ as a function of time: (a) at 5 min, (b) at 15 min, (c) at 200 min, and (d) at 630 min.
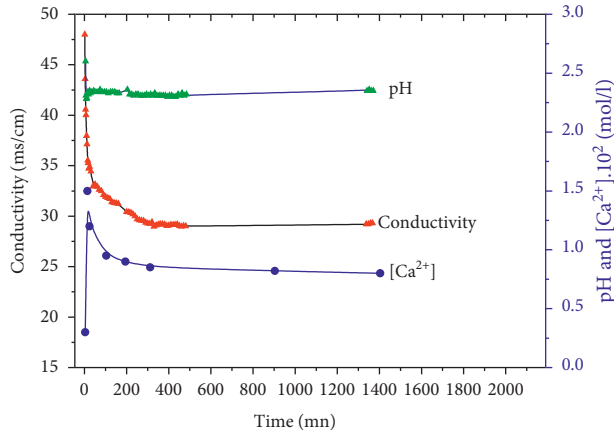
Figure 8: Evolution of the conductivity, pH, and Ca^{2+} concentration as a function of time of mixture $M4$.
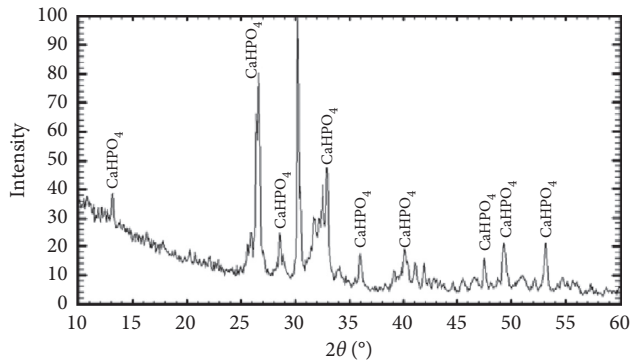

Figure 9: X-ray diffraction diagram of the solid phase formed during the precipitation of DCPA ($M4$).
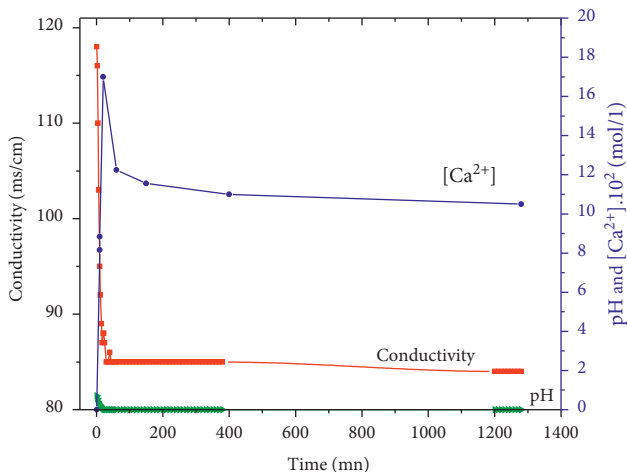

Figure 10: Variation of the conductivity, pH, and Ca^{2+} concentration of mixture $M5$ as a function of time.

The X-ray diagrams of the solid samples taken at various moments show that the formed phase corresponds to MCPM. A typical example of these diagrams is shown in Figure 11.
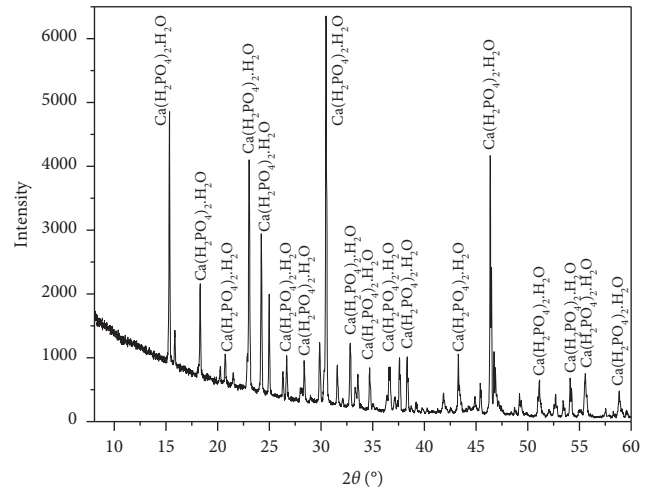

Figure 11: X-ray diffraction diagram of the solid phase formed during the precipitation of MCPM ($M5$).

Table 3: pH ranges of precipitated calcium phosphates.

Abbreviation	Chemical formula	Ca/P	Preparation conditions
Precipitates			pH
MCPM	$Ca(H_2PO_4)_2 \cdot H_2O$	0.5	0-1
DCPA	$CaHPO_4$	1	5-6
DCPD	$CaHPO_4 \cdot 2H_2O$	1	≈2.4
HAP	$Ca_{10}(PO_4)_6(OH)_2$	1.67	≈12
HAP + DCPD	—	—	7-8

4. Conclusion

In this paper, the stages of the precipitation of calcium phosphates were kinetically investigated for various mixtures by referring to the solid-liquid phase diagram of the ternary system of H_3PO_4-$Ca(OH)_2$-H_2O at 30°C [7]. The results show that, in the hydroxyapatite field, the precipitation takes place in two steps: the first consists of the formation of DCPD and HAP, while the second consists of the transformation of DCPD into HAP. In the DCPD and HAP domain, DCPD is formed in the first stage, and in the second stage, HAP is formed at the expense of part of DCPD; then, we find at the end of the precipitation a mixture of DCPD and HAP. The results also show that the precipitation of brushite passed by two stages: the first is characterized by the formation of hydroxyapatite and DCPD, whereas in the second, HAP is transformed into DCPD. The precipitation of dicalcium phosphate anhydrous (DCPA) and that of monocalcium phosphate monohydrate (MCPM) pass by a single stage.

We can conclude that the most thermodynamically stable phase does not necessarily appear first and that the studied calcium phosphates are formed at well-determined pH, as shown in Table 3.

Data Availability

The data used to support the findings of this study are included within the article.

Conflicts of Interest

The authors declare that there are no conflicts of interest regarding the publication of this paper.

References

[1] J.-C. Heughebaert, J. F. DE Rooij, and G. H. Nancollas, "The growth of dicalcium phosphate dihydrate on octacalcium phosphate at 25°C," *Journal of Crystal Growth*, vol. 76, no. 1, pp. 192–198, 1986.

[2] H. Hohl, P. G. Koutsoukos, and G. H. Nancollas, "The crystallization of hydroxyapatite and dicalcium phosphate dihydrate; representation of growth curves," *Journal of Crystal Growth*, vol. 57, no. 2, p. 325, 1982.

[3] J. F. De Rooij, J. C. Heughebaert, and G. H. Nancollas, "A ph study of calcium phosphate seeded precipitation," *Journal of Colloid and Interface Science*, vol. 100, no. 2, pp. 350–358, 1984.

[4] T. Suge, K. Ishikawa, A. Kawasaki, M. Yoshiyama, K. Asaoka, and S. Ebisu, "Effects of fluoride on the calcium phosphate precipitation method for dentinal tubule occlusion," *Journal of Dental Research*, vol. 74, no. 4, p. 1079, 1995.

[5] A. Ferreira, C. Oliveira, and F. Rocha, "The different phases in the precipitation of dicalcium phosphate dihydrate," *Journal of Crystal Growth*, vol. 252, no. 4, pp. 599–611, 2003.

[6] R. W. Marshall and G. H. Nancollas, "Kinetics of crystal growth of dicalcium phosphate dihydrate," *The Journal of Physical Chemistry A*, vol. 73, no. 14, p. 3838, 1969.

[7] K. Labgairi, A. Jourani, and M. Kaddami, "The Diffusion Coefficients of Eight Uni-univalent Electrolytes in Aqueous Solution at 25°," *Physical and Chemical News*, vol. 64, pp. 87–94, 2012.

[8] H. Chaair, I. Mansouri, and S. Nadir, "Etude de La precipitation des phosphates de calcium," *Phosphorus, Sulfur, and Silicon and the Related Elements*, vol. 170, no. 1, pp. 247–259, 2001.

[9] A. Jourani and T. Bounahmidi, "Cinétique de nucléation hétérogène et de croissance cristalline de l'hydroxyapatite lors de la précipitation spontanée des phosphates de calcium dans des solutions sucrées," *Chemical Engineering Journal*, vol. 89, no. 1-3, pp. 185–192, 2002.

[10] D. Rabadjieva, S. Tepavitcharova, K. Sezanova et al., *Biomimetic Modifications of Calcium Orthophosphates in Book: on Biomimetics*, InTech, London, UK, 2011.

[11] M. S.-A. Johnsson and G. H. Nancollas, "The role of brushite and octacalcium phosphate in apatite formation," *Critical Reviews in Oral Biology & Medicine*, vol. 3, no. 1, pp. 61–82, 1992.

[12] S. Dorozhkin, "Calcium orthophosphates in nature, biology and medicine," *Materials*, vol. 2, no. 2, pp. 399–498, 2009.

[13] L. C. Chow and E. D. Eanes, *Octacalcium Phosphate*, Karger, Basel, Switzerland, 2001.

[14] K. Labgairi, "Etude des èquilibres entre phases et de la cinètique de prècipitation des phosphates de calcium dans les conditions de lopèration dèpuration des jus de canne," *Thèse de Doctorat, université hassan 1er*, Settat, Morocco, 2015.

[15] A. Yelten-Yilmaz and S. Yilmaz, "Wet chemical precipitation synthesis of hydroxyapatite (HA) powders," *Ceramics International*, vol. 44, no. 8, pp. 9703–9710, 2018.

[16] D. Rabadjieva, K. Sezanova, R. Gergulova, R. Titorenkova, and S. Tepavitcharova, "Precipitation and phase transformation of dicalcium phosphate dihydrate in electrolyte solutions of simulated body fluids: thermodynamic modeling and kinetic studies," *Journal of Biomedical Materials Research Part A*, vol. 108, no. 8, pp. 1607–1616, 2020.